ISSN: 1410-8917
Jurnal Kimia Sains & Aplikasi
e-ISSN: 2597-9914

Jurnal Kimia Sains dan Aplikasi 25 (9) (2022): 329–337

Jurnal Kimia Sains dan Aplikasi
Journal of Scientific and Applied Chemistry

Journal homepage: http://ejournal.undip.ac.id/index.php/ksa

Preparation of Biosorbent from Kapok Fruit Peel (*Ceiba pentandra*) for Adsorption of Lead Waste

Eddy Heraldy [a,*], Novia Purnamawati [a], Arifa Zahratul Ma'wa [a], Yuniawan Hidayat [a], Khoirina Dwi Noegrahaningtyas [a], I. F. Nurcahyo [a]

[a] Department of Chemistry, Faculty of Mathematics and Natural Sciences, Sebelas Maret University, Surakarta, Indonesia

*Corresponding author: eddyheraldy@staff.uns.ac.id

https://doi.org/10.14710/jksa.25.9.329-337

Article Info

Article history:

Received: 31st July 2022
Revised: 24th October 2022
Accepted: 11th November 2022
Online: 23rd December 2022

Keywords:
Adsorption; Kapok peel fruit; *Ceiba pentandra*; lead

Abstract

The preparation of biosorbent from kapok fruit peel (KBK) for lead (Pb(II)) removal was conducted mechanically by expanding the surface of the biosorbent and activating KBK with the addition of 1 M HCl for 20 minutes. The effect of activation on increasing the number of active groups and the number of pores in the biosorbent was proven by Fourier Transform Infrared Spectroscopy (FTIR) and Scanning Electron Microscopy (SEM). The FTIR data showed a shift and an increase in wavenumber intensities of active adsorbent groups such as -OH and -C=O. The SEM data revealed that the morphology of the adsorbent increased in the number of pores that appeared rough and irregular. The Pb(II) adsorption treatment used a batch method at pH 2–5, contact time of 0–120 minutes, and adsorbate concentration of 10–50 ppm. The adsorption of Pb(II) ions reached optimum conditions at pH 4 and a contact time of 60 minutes, with an adsorption capacity of 6.9522 mg/g and an adsorption rate of 98.71%. Adsorption data showed that Pb(II) ions uptake to KBK biosorbent followed the Langmuir isotherm model equation and pseudo-second-order kinetic model. The adsorption capacity of activated KBK is greater than that of non-activated KBK.

1. Introduction

Ceiba pentandra plants are known as kapok (Indonesia), randu (Sundanese and Javanese), panju penjoi (Aceh), panji (Minangkabau), kakabu (Malay), and kapo (Madura). The part of the kapok plant that is commonly used is the fiber in its fruit, which is used as a filling material for mattresses, bolsters, or pillows. Meanwhile, the other parts of the KBK are used limitedly as a source of minerals for making soap and firewood [1].

Among the chemical components of KBK is lignocellulose, which is formed of cellulose microfibrils that form clusters, with hemicellulose filling the spaces between the microfibrils and the clusters being firmly bound by lignin [2]. A compound called cellulose has highly electron-rich hydroxyl groups. The presence of negatively charged hydroxyl groups in KBK allows for electrostatic interactions with positively charged metal ions so that KBK has the potential to act as a biosorbent to adsorb heavy metals. According to Kayranli [3], biosorbents containing lignin, cellulose, and hemicellulose have functional groups such as –OH,–COOH, –OH, $-CH_3$, $-NO_2$, $-CH_2$, –CH, amino acids, and others, which are involved in removing a heavy metal process.

The synthesis of KBK as an adsorbent has not been widely reported, although several researchers have used it to remove dyes and heavy metals. Zhang *et al.* [4] have utilized kapok fiber to absorb cationic dyes as an inexpensive, environmentally friendly adsorbent. Other researchers, Astuti *et al.* [5], have utilized *C. pentandra* powder as a biosorbent using sodium hydroxide activator to increase its adsorption capacity in removing methyl violet dye. However, until now, not many researchers have used kapok peel as a biosorbent using an acid activator. Rao *et al.* [6] have prepared its biosorbent by making activated carbon without activator treatment. Likewise, in the study reported by Zein *et al.* [7], the activator was used as nitric acid. In addition, research conducted by Adeko and Mualim [8] used KBK biosorbents to determine the adsorption capacity of Fe.

This study investigated the hydrochloric acid-preactivated KBK biosorbent preparation technique. The performance of the biosorbent formulations was then evaluated concerning the adsorption of Pb(II). Pb(II) in wastewater primarily originates from the production of metal painting and finishing, battery manufacturing, soldering materials, printing and pigments, glass and ceramics, ammunition, steel, and iron manufacturing units [9]. Because of their natural propensity for toxicity, persistence, bioaccumulation, and non-biodegradable, heavy metal ions like Pb(II) must be removed from wastewater [10, 11]. Lead poisoning also causes reproductive disorders, damage to the central nervous system, and physical and psychological problems–especially in children [12]. In addition, its potential carcinogenic and neurologic effects can lead to death [13].

Therefore, efforts to remove Pb(II) ions through the adsorption process continue to be carried out by the research team with different biosorbents [14]. The adsorption process was studied through the Langmuir and Freundlich isotherm model, which is related to the interaction of several adsorbates on the surface of the adsorbent and determined the type of adsorption that occurred. Another aspect studied was the adsorption kinetics to determine the adsorption rate of the adsorbent on the adsorbate.

2. Methods

2.1. Materials and equipment

The materials used in this study were KBK (*Ceiba pentandra*), HCl (Merck), HNO_3 (Merck), NaOH (Merck), $Pb(NO_3)_2$, filter paper (Whatman 42), universal indicator (Merck), and distilled water. The equipment used was Atomic Absorption Spectroscopy (AAS) Shimadzu type AA-6650 F, Fourier Transform-Infra Red (FT-IR) Shimadzu type FT-IR-8201 PC, Scanning Electron Microscope (SEM) type JSM-6510, blender, hot plate, stirrer, furnace, electrical analytical balance, pH meter, magnetic stirrer, 150 mesh size sieve, and glasswares (Pyrex).

2.2. Preparation of biosorbent

The peel of the kapok fruit was washed thoroughly under running water until the KBK sample became clean and free of dirt adhering to it, then dried to remove gum so it would be easy to process. After that, the KBK sample was mechanically crushed into powder that passed a 150 mm sieve [7]. The activation of the biosorbent was prepared by placing the KBK powder into a beaker and then adding 1 M HCl at a ratio of 1:30 (w/v) and allowing it to stand for 20 minutes. The solution was filtered, and the residue was dried in an oven at 60℃ for 24 hours. The remaining powder clumps were ground using a blender and sifted through a 150-mesh sieve. The sieved powder (activated biosorbent) was characterized using FTIR to identify functional groups and SEM to determine surface morphology.

2.3. Effectiveness test of biosorbent

KBK powder (0.1 g) was added to 15 mL of 50 ppm Pb(II) solution, which had been adjusted using HCl and NaOH to achieve pH 2, 3, 4, and 5, with continuous shaking for different contact times of 15, 30, 60, 90, and 120 minutes. The obtained solutions were filtered using Whatman 42 filter paper, and the volume after adsorption was measured. The concentration of Pb(II) ions in the filtrate were determined using AAS. The performance of KBK adsorbent can be determined by making a relationship curve between pH and contact time with the percentage of adsorbed Pb(II) ions. After adsorption, the KBK biosorbent was characterized using FT-IR and SEM.

2.4. Determination of adsorption isotherms

KBK powder (0.1 g) was added into each flask containing Pb(II) ion solution of various concentrations (10, 20, 30, 40, and 50 ppm) and then stirred at optimum contact time. The solutions were filtered, and Pb(II) concentrations were determined using AAS. The results were then calculated using the Langmuir and Freundlich isotherm model equations (1) and (2), respectively [14].

$$\frac{C_e}{q_e} = \frac{C_e}{q_m} + \frac{1}{K_L.q_m} \quad (1)$$

$$\ln q_e = \ln K_F + \frac{1}{n} \ln C_e \quad (2)$$

where, q_e is the amount of adsorbed Pb(II) ions per amount of adsorbent (mg/g), C_e is the equilibrium concentration of Pb(II) ions (mg/L), q_m is the amount of adsorbate required to form monolayers (mg/g), and K_L is Langmuir equilibrium constant (L/mg), K_F and $1/n$ are Freundlich isotherms for adsorption of Pb(II) ions.

2.5. Determination of adsorption kinetics

KBK powder (0.1 g) was added into each flask containing 15 mL of Pb(II) ions solution of 50 ppm at preadjusted pH. The solutions were stirred continuously for 15, 30, 60, 90, and 120 minutes under constant pH conditions. The obtained mixtures were then filtered using Whatman 42 filter paper, and the volume after adsorption was measured. The concentration of Pb(II) ions in the filtrate were determined using AAS. The adsorption rate equation models are first-order, second-order, pseudo-first-order, and pseudo-second-order. The following is an example of a pseudo-first-order (3) and all-second-order (4) equations model for determining reaction kinetics.

$$\log(q_e - q_t) = \log q_e - \frac{k_1}{2.303} t \quad (3)$$

where, q_e is the amount of solute adsorbed per unit biosorbent mass at equilibrium (mg/g), q_t is the amount of solute adsorbed at any time (mg/g), and k_1 is the apparent first-order rate constant.

$$\frac{t}{q_t} = \frac{1}{k_2 q_e^2} + \frac{1}{q_e} t \quad (4)$$

where, k_2 is the pseudo-second-order rate constant (g/(mg min)), t is adsorption time (min), q_e is the adsorption capacity of Pb(II) ion from the biosorbent at equilibrium (mg/g), and q_t is the adsorption capacity at time t (mg/g). The k_2 and q_e are obtained from the slope ($1/q_e$) and intercept $1/ k_2.q_e^2$)) of the t / q_t versus t linear plot.

3. Results and Discussion

3.1. Biosorbent activation

The adsorption capacity of the biosorbent was improved by the activation process of adding 1 M HCl solution such that the surface acidity increased optimally as a result of the exchange of H^+ ions with cations from salts and minerals in KBK. The Cl^- from HCl binds impurities, allowing the active sites (-OH and -COOH) to interact with the adsorbate more easily. The activation results are shown in Figure 1, where KBK powder was brownish-yellow and reddish-brown after activation.

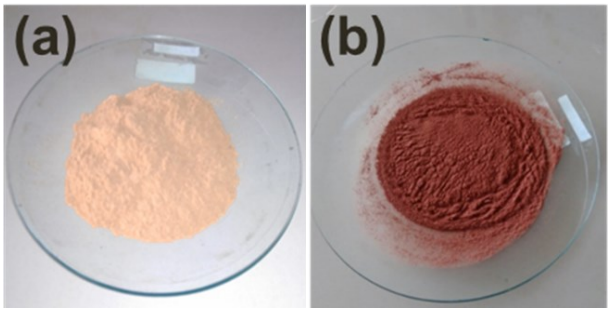

Figure 1. Kapok peel powder (a) before activation and (b) after activation

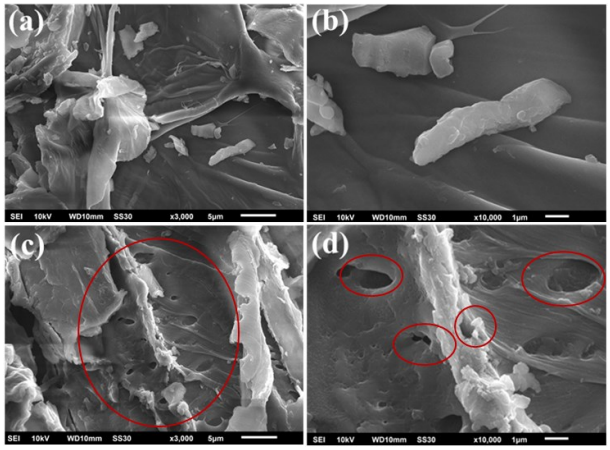

Figure 2. SEM images of KBK biosorbent (a) without treatment at 3000× magnification, (b) without treatment at 10,000× magnification, (c) activated at 3000× magnification, (d) activated at 10,000× magnification

The results of SEM characterization are shown in Figure 2, which clearly shows the surface morphologies of KBK before and after activation. Figures 2(a) and 2(b) show that the morphology of the KBK biosorbent before activation is a relatively flat surface, and the pores are still closed and non-hollow. The activation process is proven to dissolve impurities so that many pores appear on the surface, as shown in Figures 2(c) and 2(d). The active groups of the biosorbent component are more open, allowing the adsorbate to fill the space on the surface. This is confirmed by the FTIR analysis shown in Figure 3.

The FTIR spectra in Figure 3(a) reveal that KBK exhibits a stretching vibration of the OH group at the peak of 3385 cm^{-1}, which in this wavelength range indicates the presence of intramolecular hydrogen bonds and is the main group in cellulose [9]. The wavenumber 2915 cm^{-1} shows the characteristic CH stretching in cellulose. The OH bending vibrations of water absorbed in the cellulose are visible in the 1730 cm^{-1} region. The characteristics of the CC stretching are found in the absorption area of 1057 cm^{-1}. Absorption at 1433 cm^{-1} reveals the presence of $-CH_2$ bending in cellulose, indicating the existence of a crystalline region. The band at 1143 cm^{-1} corresponds to the C-O-C ring stretching vibration of the β-glycosidic bond, whereas the peak at 895-897 cm^{-1} corresponds to the CH stretching of the β-glycosidic in cellulose. The presence of a lignin component is indicated by a peak of skeletal aromatic vibrations between 1200 and 1300 cm^{-1}, which is seen as a peak at 1254 cm^{-1} in the spectra. The absorption bands at 1254 and 1519 cm^{-1} are related to the C=C bending in lignin. The presence of hemicellulose is proven by the appearance of C=O absorption groups in the 1612 cm^{-1} region.

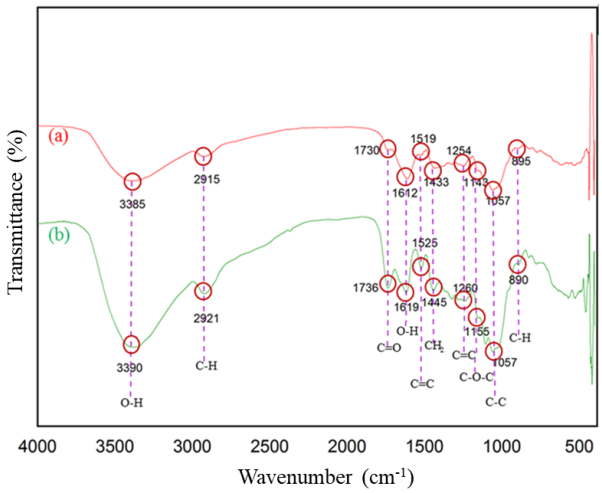

Figure 3. FTIR spectra of KBK biosorbent (a) before activation and (b) after activation

The FTIR spectra in Figure 3(b) demonstrate that the activation process significantly affected the KBK biosorbent. The data in Table 1 suggests that the absorption of the -OH group stretching vibration experience peak broadening. The sharpening of the absorption peak of the -OH group and other active groups after activation indicates an increase in absorption intensity. The stretching vibrations of C-H, C=O, C=C, and C-O-C, the bending vibrations of -OH and $-CH_2$, and the aromatic ring of C-C were among the other groups that reported an increase in absorption intensity. The increase in intensity is possible since the activation has eliminated the contaminants. Simultaneously removing impurities from the adsorbent surface, the C-H absorption peak of β-glycosidic in cellulose decreased in intensity but did not eliminate the absorption of functional groups.

Table 1 reveals the difference between the KBK before and after activation as a shift in wavenumbers that change absorption intensity due to removing the contaminants after the activation process. The activation process will enlarge existing pores formed on the surface of the KBK, making the functional groups that comprise the biosorbent more active. The results of the FTIR analysis showed that the KBK biosorbent has active C=O and –OH lignocellulosic functional groups that can contribute to the adsorption of heavy metals.

Table 1. Comparison of FTIR of KBK adsorption before and after activation

No	Functional groups	Wavenumbers (cm^{-1})		
		References	Before Activation	After Activation
1	O-H (stretching)	3320 [7]	3385	3390
2	C-H (stretching)	2928 [15]	2915	2921
3	C=O	1728 [16]	1730	1736
4	-OH (bending)	1611 [15]	1612	1619
5	C=C (stretching)	1400-1600 [7]	1519	1525
6	$-CH_2$ (bending)	1437 [17]	1433	1445
7	C=C aromatic ring	1250 [15]	1254	1260
8	C-O-C (stretching)	1100 [16]	1143	1155
9	C-C (stretching)	1057 [17]	1057	1057
10	C-H (stretching)	895 [15]	895	890

Table 1 reveals the difference between the KBK before and after activation as a shift in wavenumbers that change absorption intensity due to removing the contaminants after the activation process. The activation process will enlarge existing pores formed on the surface of the KBK, making the functional groups that comprise the biosorbent more active. The results of the FTIR analysis showed that the KBK biosorbent has active C=O and –OH lignocellulosic functional groups that can contribute to the adsorption of heavy metals.

3.2. Adsorption performance on Pb(II)

The adsorption capacity of KBK was determined by adsorbing Pb(II) under various adsorption conditions. The pH of the solution and contact time were the two parameters optimized for the adsorption conditions.

3.2.1. Optimization of pH variation

The result for optimization of pH variation can be seen in Figure 4. The pH solution can influence the adsorption process because, at low pH, metal ions and H^+ ions will compete for binding to the active site of the biosorbent. H^+ ions may bind to the active site of the biosorbent [18, 19].

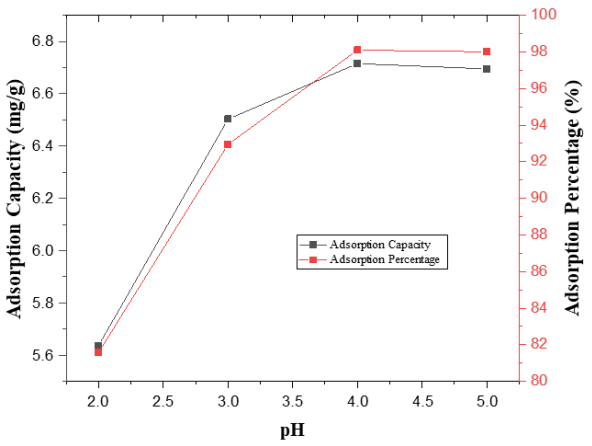

Figure 4. The curve of the effect of pH variations on adsorption capacity and percentage of Pb(II) ion adsorption

The optimum pH condition for the adsorption of Pb(II) ions was 4, with an adsorption capacity of 6.7152 mg/g and an adsorption percentage of 98.10%. It is known from the curve in Figure 4 that increasing the pH to 4 can enhance adsorption capacity. This can be caused by the biosorbent surface being surrounded by H^+ ions at low pH resulting in protonation, which leads the biosorbent surface to become more positively charged [19].

The lowest adsorption capacity of Pb(II) ions on the KBK biosorbent was at pH 2 due to competition between H^+ ions and Pb(II) ions in binding to the surface of the KBK biosorbent. The presence of excess H^+ ions has the potential to replace Pb(II) ions to bind to the surface active sites of the biosorbent, resulting in Pb(II) ions not being adsorbed by the KBK biosorbent. The adsorption capacity of Pb(II) ions enhanced with increasing pH, especially at pH 3 and 4, as a result of Pb(II) ions binding to the active sites of the adsorbent, which subsequently formed $Pb(OH)_2$. The adsorption capacity began to decrease at pH 5—the solution approaches base conditions—due to the formation of lead hydroxide precipitates, thus limiting the KBK biosorbent from adsorbing all of the Pb(II) ions.

3.2.2. Optimization of contact time variations

The optimal contact time was obtained after the biosorbent and adsorbate reached equilibrium. According to Figure 5, it is known that the optimum contact time for Pb(II) metal ion adsorption occurs at a contact time of 60 minutes with an adsorption capacity of 6.9522 mg/g and an adsorption percentage of 98.71%. According to the obtained data, the adsorption capacity of biosorbent increased with increasing contact time. However, after the optimal contact time has been reached, the adsorption capacity will stabilize and decrease. This is because the amount of adsorbate that binds to the biosorbent is already saturated, so the additional adsorption time will lead to desorption or re-releasing of the adsorbate from the biosorbent [7]. Consequently, it appears that the Pb(II) ion on the biosorbent becomes saturated, which will cause a desorption process that will result in the formation of free Pb in the solution.

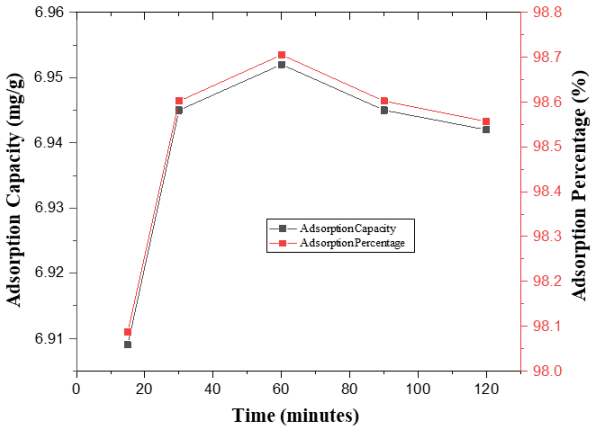

Figure 5. The curve of the effect of contact time on adsorption capacity and percentage of Pb(II) metal ion adsorption

3.3. Characterization of KBK biosorbent after adsorption

The FTIR spectra profile comparing the FTIR spectra before and after the adsorption process is shown in Figure 6(c). Unactivated KBK biosorbent had an adsorption capacity of 6.5883 mg/g and an adsorption efficiency of 93.54%. Adsorption increased significantly after activation. The activated KBK biosorbent had an adsorption capacity of 6.9522 mg/g and an adsorption efficiency of 98.71%.

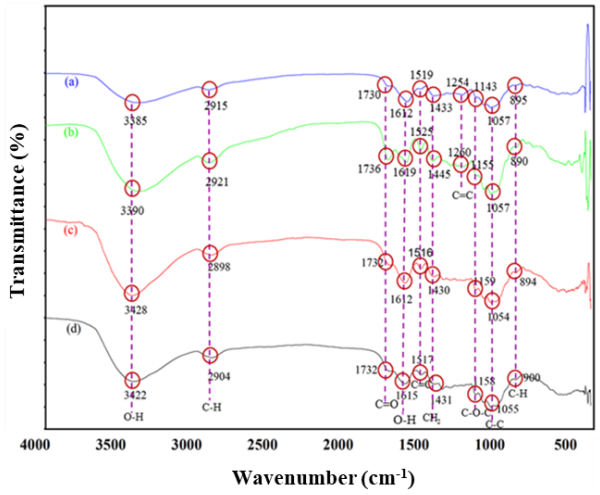

Figure 6. FTIR spectra profile of biosorbent (a) before activation, (b) after activation, (c) after Pb(II) ion adsorption

Based on the data obtained from the FTIR characterization before and after adsorption in Table 2, there was a shift in the wavenumber of the biosorbent's functional group before and after adsorption at 3390 cm^{-1} to 3428 and 3422 cm^{-1} which was the absorption of the -OH groups.

Table 2. Comparison of FTIR absorption of KBK biosorbent before and after activation and after Pb(II) ion adsorption

No.	Functional groups	Wavenumber (cm^{-1})		
		References	Before Adsorption	After Adsorption
1	O-H (stretching)	3320 [7]	3390	3428
2	C-H (stretching)	2928 [15]	2921	2898
3	C=O	1728 [16]	1736	1732
4	-OH (bending)	1611 [15]	1619	1612
5	C=C (stretching)	1400-1600 [7]	1525	1516
6	$-CH_2$ (bending)	1437 [17]	1445	1430
7	C=C aromatic ring	1250 [15]	1260	-
8	C-O-C (stretching)	1100 [16]	1155	1159
9	C-C (stretching)	1057 [17]	1057	1054
10	C-H (stretching)	895 [15]	890	894

The data in Table 2 showed that the intensity of the active groups of the biosorbent decreased after the adsorption of Pb(II) metal ions. The shift of the absorption area from 1736 cm^{-1} to 1732 cm^{-1} represents a C=O absorption. The intensity decreases as the bond gets stronger because it becomes more difficult for vibrations to occur. A higher wavenumber shift suggests an increase in bond strength, whereas a lower one indicates a reduced bond strength [20]. This shift is possible due to the interaction of the active group with Pb(II) metal ions. This indicates an interaction between functional groups such as OH and C=O with heavy metal ions, causing the bond energy to become stronger. The mechanism of metal ion adsorption by KBK biosorbent has several possible mechanisms, including ion exchange, complex formation, and adsorption by diffusion. According to Tangio [21], the adsorption reaction via ion exchange occurs as described by equation (1).

$$2[S-H] + Pb^{2+} \leftrightarrow S_2Pb + 2H^{+} \quad (1)$$

where, S–H is the surface site of the biosorbent involved in the adsorption process, Pb^{2+} is the equilibrium concentration of metal ions, and S–M represents the metal adsorbed on the biomass.

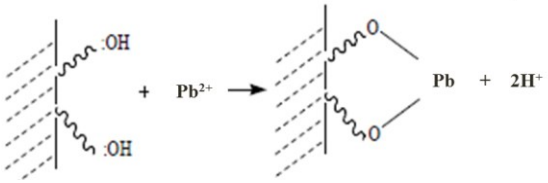

Figure 7. Interaction mechanism between active groups of biosorbent and Pb(II) ions [22]

Adsorption is affected by ion exchange reactions involving metal ions and functional groups in the adsorbent. Figure 7 depicts the ion exchange mechanism in which the Pb(II) cation replaces the H^{+} ion in the hydroxyl and carboxylic groups. Deprotonation of the functional group (-OH or -COOH) with the metal generates an electrostatic force that drives the ion exchange adsorption process [23]. Due to the formation of complexes, the adsorption process occurs between heavy metal ions and functional groups, such as carbonyl, hydroxyl, and carboxyl. The adsorption process that occurs is reversible and rapid [24].

The possibility of a metal ion adsorption mechanism by KBK biosorbent also occurs through physisorption. The Pb(II) ion may be adsorbed through the adsorption mechanism since it has a size of 1.12 Å. Adsorption that occurs by physisorption does not involve chemical reactions or changes in chemical properties. This interaction involves weak Van der Waals forces between the adsorbent surface and the adsorbate molecules. The presence of this force causes metal molecules to be adsorbed by diffusion into the pores of the biosorbent [25]. Since the pore diameter of biosorbents is typically 2 nm ≤ Dp ≥ 50 nm, smaller Pb(II) ions can be adsorbed into the biosorbent pores [26]. Physisorption of Pb(II) ions is the predominant process supported by FTIR analysis.

3.4. Determination of adsorption isotherms

The Langmuir and Freundlich isotherm method was used to determine the adsorption isotherm in order to observe the equilibrium relationship between the adsorbate concentration in the liquid phase and the adsorbate concentration on the adsorbent surface at a particular temperature [14]. The results of the Langmuir isotherm of KBK biosorbent in Pb(II) ions at pH 4 and a contact time of 60 minutes are shown in Figure 8.

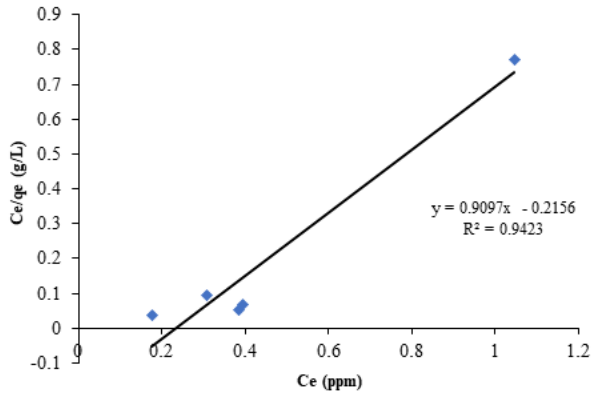

Figure 8. Langmuir isotherm curve of KBK biosorbent in Pb(II) ions

Increasing the adsorbate concentration increases the adsorption capacity linearly as long as the active sites on the surface are not saturated with the adsorbate. However, if the active site contained in the adsorbate is saturated, further concentration will not increase the amount of adsorbate being adsorbed. Determination of the type of adsorption isotherm is obtained from the correlation coefficient (R^2) from the linear equation graph of each adsorption isotherm curve.

The type of isotherm follows the equation if the R^2 value of the adsorption isotherm equation is close to or equal to 1 (one). The adsorption process between the adsorbent and the adsorbate based on the Langmuir isotherm occurs chemically, namely between the active groups of the adsorbent interacting with Pb(II) ions through chemical bonds. According to Langmuir, the adsorption process between the adsorbent and the adsorbate is limited and forms a single layer.

The Freundlich adsorption isotherm curve of KBK biosorbent in Pb(II) ions is shown in Figure 9. The adsorption process between the adsorbent and the adsorbate based on the Freundlich isotherm occurs physically through the Van der Waals force. Van der Waals force occurs because the electropositive adsorbate interacts with the electronegative adsorbent. Adsorption that occurs by physisorption causes the physically adsorbed molecules to be weakly bound to the surface, and a fast reversible process occurs, thus easily replacing them with other molecules [27]. The positively charged Pb(II) ions will interact with the negatively charged O atom, so the distance between the Pb(II) ion and the O atom becomes closer due to the presence of dipoles. The adsorbent and the adsorbate interact through Pb(II) ions sticking to the pores of the adsorbent with a weak binding energy through the Van der Waals force. The attractive force that occurs causes the adsorbate to move from one part of the adsorbent surface to another to form a multilayer.

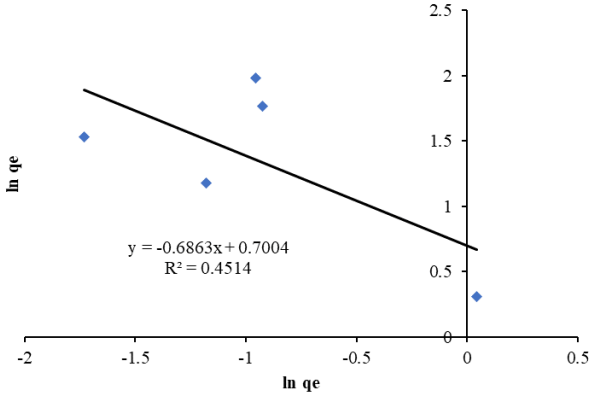

Figure 9. Freundlich isotherm curve of KBK biosorbent in Pb(II) ions

The data obtained from Langmuir and Freundlich isotherms of KBK biosorbent in Pb(II) ions are shown in Table 3. Based on Table 3, the determination of the adsorption isotherm of Pb(II) ions yields an R^2 value for the Langmuir isotherm of 0.9423 with an adsorption capacity of 1.0993 mg/g and an R^2 value for the Freundlich isotherm of 0.4514 with an adsorption capacity of 2.0146 mg/g. The R^2 value of the Langmuir isotherm is closer to 1 than that of the Freundlich isotherm, but the adsorption capacity of Pb(II) metal ions is greater in the Freundlich isotherm. In conclusion, the adsorption process of Pb(II) ions follows the Langmuir and Freundlich isotherms and has a relative tendency to the Langmuir isotherm.

Table 3. Langmuir and Freundlich isotherm data

Isotherms	Parameters	Pb(II)
Langmuir	q_m (mg/g)	1.0093
	R^2	0.9423
Freundlich	K_f (mg/g)	2.0146
	n	-1.4571
	R^2	0.4514

3.5. Determination of adsorption kinetics

A determination of adsorption kinetics was conducted to determine the rate of adsorbate adsorption [28]. The models of adsorption kinetics equations that were tested included first-order, second-order, pseudo-first-order, and pseudo-second-order equation models. All Pb(II) ions adsorption kinetics models are presented in Figure 10.

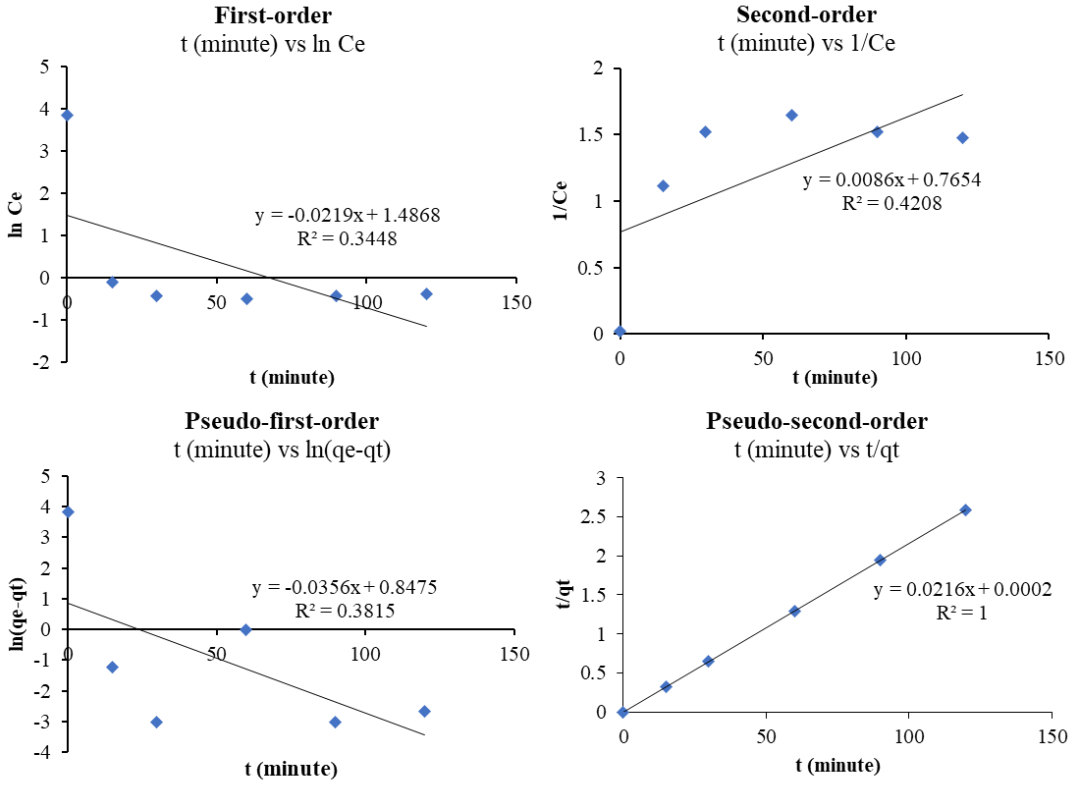

Figure 10. The plot of the kinetic models of Pb(II) ions adsorption sequentially (first-order, second-order, pseudo-first-order, pseudo-second-order)

Table 4. Parameters of first-order, second-order, pseudo-first-order, and pseudo-second-order adsorption kinetics

Kinetic models	Parameters	Pb(II)
First-order	*k*	0.0219
	R^2	0.3448
Second-order	*k*	0.0086
	R^2	0.4208
Pseudo-first-order	*k*	0.0356
	R^2	0.3815
Pseudo-second-order	*k*	2.3328
	R^2	1.0000

The adsorption kinetics data is shown in Table 4. The adsorption kinetics model for the appropriate Pb(II) ions system was determined by comparing the R^2 values. The kinetic equation model is selected based on the R^2 value closest to one. Based on the obtained data, the kinetic model of the adsorption of Pb(II) ions by the KBK biosorbent is a pseudo-second-order kinetics model. The reaction between the adsorbent and the adsorbate in the pseudo-second-order kinetic model is identical to the chemical reaction. The pseudo-second-order kinetics model is suitable for most adsorption for the overall contact time, which lasts longer, and the removal rate is high [28]. The value of *k* indicates the magnitude of the adsorption rate. The value of *k* is directly proportional to the rate of adsorption.

4. Conclusion

The characteristics of the KBK biosorbent after activation underwent significant changes. FTIR and SEM characterization of kapok peel showed an increase in the absorption intensity of the active group after activation. The optimum conditions for Pb(II) adsorption on KBK biosorbent were pH of 4, contact time of 60 minutes with an adsorption capacity of 6.9522 mg/g, and an adsorption percentage of 98.71%. The adsorption process follows the Langmuir isotherm and pseudo-second-order kinetics, so chemical and physical interactions occur during the adsorption process.

Acknowledgment

Thank you to Sebelas Maret University for funding this research with a Fundamental Grant Scheme for 2021-2022.

References

[1] Renny Purnawati, Fauzi Febrianto, I. Wistara, Siti Nikmatin, Wahyu Hidayat, Seunghwan Lee, Namhun Kim, Physical and chemical properties of kapok (*Ceiba pentandra*) and balsa (*Ochroma pyramidale*) fibers, *Journal of the Korean Wood Science and Technology*, 46, 4, (2018), 393-401 https://doi.org/10.5658/WOOD.2018.46.4.393

[2] Muhammad Faizal, Achmad Daniel Rifky, Irwanto Sanjaya, Pembuatan briket dari campuran limbah plastik LDPE dan kulit buah kapuk sebagai energi alternatif, *Jurnal Teknik Kimia*, 24, 1, (2018), 8-16

[3] Birol Kayranli, Mechanism of interaction and removal of zinc with lignocellulosic adsorbents, closing the cycle with a soil conditioner, *Journal of King Saud University-Science*, 33, 8, (2021), 101607 https://doi.org/10.1016/j.jksus.2021.101607

[4] Xiulan Zhang, Chunting Duan, Xin Jia, Bin Dai, Carboxylation kapok fiber as a low-cost, environmentally friendly adsorbent with remarkably enhanced adsorption capacity for cationic dyes, *Research on Chemical Intermediates*, 42, 5, (2016), 5069-5085 https://doi.org/10.1007/s11164-015-2345-2

[5] W. Astuti, T. Sulistyaningsih, M. Maksiola, Equilibrium and Kinetics of Adsorption of Methyl Violet from Aqueous Solutions Using Modified *Ceiba pentandra* Sawdust, *Asian Journal of Chemistry*, 29, 1, (2017), 133-138 https://doi.org/10.14233/ajchem.2017.20158

[6] M. Madhava Rao, G. P. Chandra Rao, K. Seshaiah, N. V. Choudary, M. C. Wang, Activated carbon from *Ceiba pentandra* hulls, an agricultural waste, as an adsorbent in the removal of lead and zinc from aqueous solutions, *Waste Management*, 28, 5, (2008), 849-858 https://doi.org/10.1016/j.wasman.2007.01.017

[7] Rahmiana Zein, Dewi Nofita, Refilda Refilda, Hermansyah Aziz, Penyerapan Timbal (II) dan Cadmium (II) di dalam Larutan Menggunakan Limbah Kulit Buah Kapuk, *Chimica et Natura Acta*, 7, 1, (2019), 37-45 https://doi.org/10.24198/cna.v7.n1.20813

[8] City Riang Adeko, Mualim Mualim, Kombinasi limbah sekam padi dan limbah kulit kapuk sebagai adsorben dalam menurunkan kadar besi (Fe) di sumur gali warga rawa makmur kota Bengkulu (Combination of rice husk waste and kapuk skin waste as an adsorben in reducing iron (Fe) levels in the wells of well rawa makmur citizens in Bengkulu city), *Journal of Nursing and Public Health*, 8, 1, (2020), 97-103

[9] Tariq Mahmood Ansari, Muhammad Asif Hanif, Abida Mahmood, Uzma Ijaz, Muhammad Aslam Khan, Raziya Nadeem, Muhammad Ali, Immobilization of rose waste biomass for uptake of Pb(II) from aqueous solutions, *Biotechnology Research International*, 2011, 685023, (2011), 1-9 https://doi.org/10.4061/2011/685023

[10] Madala Suguna, Nadavala Siva Kumar, Vudagandla Sreenivasulu, Abburi Krishnaiah, Removal of Pb(II) from aqueous solutions by using chitosan coated zero valent iron nanoparticles, *Separation Science and Technology*, 49, 10, (2014), 1613-1622 https://doi.org/10.1080/01496395.2014.901361

[11] Reza Tabaraki, Ashraf Nateghi, Salman Ahmady-Asbchin, Biosorption of lead (II) ions on *Sargassum ilicifolium*: application of response surface methodology, *International Biodeterioration & Biodegradation*, 93, (2014), 145-152 https://doi.org/10.1016/j.ibiod.2014.03.022

[12] D. Harikishore Kumar Reddy, Y. Harinath, K. Seshaiah, A. V. R. Reddy, Biosorption of Pb(II) from aqueous solutions using chemically modified *Moringa oleifera* tree leaves, *Chemical Engineering Journal*, 162, 2, (2010), 626-634 https://doi.org/10.1016/j.cej.2010.06.010

[13] Bruno L. Martins, Claudio C. V. Cruz, Aderval S. Luna, Cristiane A. Henriques, Sorption and desorption of Pb^{2+} ions by dead *Sargassum* sp. biomass, *Biochemical Engineering Journal*, 27, 3, (2006), 310-314 https://doi.org/10.1016/j.bej.2005.08.007

[14] Eddy Heraldy, Witri Wahyu Lestari, Diah Permatasari, Devita Dwi Arimurti, Biosorbent from tomato waste and apple juice residue for lead removal, *Journal of Environmental Chemical Engineering*, 6, 1, (2018), 1201-1208 https://doi.org/10.1016/j.jece.2017.12.026

[15] Axel Gian Aditama, Hosta Ardhyananta, Isolasi Selulosa dari Serat Tandan Kosong Kelapa Sawit untuk Nano Filler Komposit Absorpsi Suara: Analisis FTIR, *Jurnal Teknik ITS*, 6, 2, (2017), F229-F232 http://dx.doi.org/10.12962/j23373539.v6i2.24098

[16] Tristan Petit, Ljiljana Puskar, FTIR spectroscopy of nanodiamonds: Methods and interpretation, *Diamond and Related Materials*, 89, (2018), 52-66 https://doi.org/10.1016/j.diamond.2018.08.005

[17] Abdullah Chandra Sekhar Talari, Marcela A. Garcia Martinez, Zanyar Movasaghi, Shazza Rehman, Ihtesham Ur Rehman, Advances in Fourier transform infrared (FTIR) spectroscopy of biological tissues, *Applied Spectroscopy Reviews*, 52, 5, (2017), 456-506 https://doi.org/10.1080/05704928.2016.1230863

[18] K. S. Low, C. K. Lee, K. P. Lee, Sorption of copper by dye-treated oil-palm fibres, *Bioresource Technology*, 44, 2, (1993), 109-112 https://doi.org/10.1016/0960-8524(93)90183-C

[19] Bouamama Abbar, Abdellah Alem, Stéphane Marcotte, Anne Pantet, Nasre-Dine Ahfir, Laurent Bizet, Davy Duriatti, Experimental investigation on removal of heavy metals (Cu^{2+}, Pb^{2+}, and Zn^{2+}) from aqueous solution by flax fibres, *Process Safety and Environmental Protection*, 109, (2017), 639-647 https://doi.org/10.1016/j.psep.2017.05.012

[20] Abu Masykur, Nurul Fatimah, Santika Kunti Prabawani, Fabrication of Sugar Palm Fiber/Andisol Soil Composites for Iron (III) ion Removal in Aqueous Solution, *Oriental Journal of Chemistry*, 34, 1, (2018), 346 http://dx.doi.org/10.13005/ojc/340137

[21] Julhim S. Tangio, Adsorpsi logam timbal (Pb) dengan menggunakan biomassa enceng gondok (*Eichhorniacrassipes*), *Jurnal Entropi*, 8, 1, (2013),

[22] Riska Kusumawardani, Titin Anita Zaharah, Lia Destiarti, Adsorpsi kadmium(II) menggunakan adsorben selulosa ampas tebu teraktivasi asam nitrat, *Jurnal Kimia Khatulistiwa*, 7, 3, (2018), 75-83

[23] Avander Alexander Nuban, Anna Safitri, Ulfa Andayani, Biosorption of Lead (Pb) from Aqueous Solution by Immobilized Aspergillus niger: A Green Technology for Heavy Metals Removal, *The Indonesian Green Technology Journal*, 10, 1, (2021), 21-27

[24] A. W. Nugraha, O. Suparno, N. S. Indrasti, Utilization of rice husk as a tanning agent in the tanning process of leather (A mini review), *IOP Conference Series: Earth and Environmental Science*, 2019 https://doi.org/10.1088/1755-1315/335/1/012032

[25] Citra Dewi Rakhmania, Indah Khaeronnisa, Bambang Ismuyanto, Julia Nanda, Nurul Faiqotul Himma, Adsorpsi Ion Kalsium Menggunakan Biomassa Eceng Gondok (*Eichhornia crassipes*) Diregenerasi HCl, *Jurnal Rekayasa Bahan Alam dan Energi Berkelanjutan*, 1, 1, (2017), 16-24 https://doi.org/10.21776/ub.rbaet.2017.001.01.03

[26] Fajar Indah Puspita Sari, Ristika Oktavia Asriza, Biosorben Kulit Jengkol (*Pithecellobium jiringa*) sebagai Penyerap Logam Pb pada Air Kolong Pasca Penambangan Timah, *Jurnal Sains Teknologi & Lingkungan*, 4, 2, (2018), 83-89 https://doi.org/10.29303/jstl.v4i2.81

[27] Hesti Apriyanti, I Nyoman Candra, Elvinawati Elvinawati, Karakterisasi isoterm adsorpsi dari ion logam besi (Fe) pada tanah di kota Bengkulu, *Alotrop*, 2, 1, (2018), 14-19 https://doi.org/10.33369/atp.v2i1.4588

[28] Martin A. Hubbe, Saeid Azizian, Sigrid Douven, Implications of apparent pseudo-second-order adsorption kinetics onto cellulosic materials: A review, *BioResources*, 14, 3, (2019), 7582-7626 https://doi.org/10.15376/BIORES.14.3.7582-7626